2008 IEEE International Conference on
Robotics and Automation
Pasadena, CA, USA, May 19-23, 2008

Optimal Jumps for Biarticular Legged Robots

Bokman Lim, J. Babič, and F.C. Park

Abstract— **This paper investigates the extent to which biarticular actuation mechanisms—antagonistic actuation schemes with spring stiffness that extend over two joints, similar in function to biarticular muscles found in legged animals—improve the performance of jumping and other fast explosive robot movements. Robust gradient-based optimization algorithms that take into account the dynamic properties and various contact and actuator constraints of biarticular systems are developed. We then quantitatively evaluate the gains in jumping vis-à-vis conventional joint actuation schemes. We also examine the effects of biarticular link stiffness and link mass distributions on the jumping performance of the biarticular mechanism.**

Index Terms— **Legged robot, biarticular muscle, movement optimization, jumping.**

I. Introduction

Although recent biped robots have displayed impressive movement coordination skills that require balance and dexterity, as of yet none can even remotely approach the ability of humans to jump, run, kick, or perform other fast, explosive movements. Several studies on jumping have been undertaken for one degree-of-freedom mechanisms [1], [2], and for jumping robots with multiple degrees of freedom [3], [4]. Computationally intensive numerical optimization-based studies of hopping and vertical jumping have also been performed [5], [6], which take into account models for the ground-foot contact, actuators, and multibody dynamics (of the human musculoskeletal system in the latter case), and numerically determine optimal jumps based on, *e.g.*, user-specified center-of-mass trajectories, contact time, air time, take-off time.

One intriguing attempt at addressing the limitations of current actuators can be found in schemes that emulate the properties of biarticular muscles such as those found in human legs. These antagonistic muscles extend over two joints—the human gastrocnemius muscle, for example, extends from the knee to the ankle joints, and acts as both a knee flexor and ankle extensor (Figure 1)—and have been found to play a critical role in the generation of fast explosive human movements [7]. The gastrocnemius muscle also has the interesting feature of being connected to the foot by an elastic tendon; several biomechanical studies have confirmed the importance of elasticity in the tendons and muscle fibers in enhancing, *e.g.*, jumping and running motions [8], [9].

Bokman Lim and F.C. Park are with the School of Mechanical and Aerospace Engineering, Seoul National University, Korea. bokman2@robotics.snu.ac.kr, fcp@snu.ac.kr

J. Babič is with the Department of Automatics, Biocybernetics and Robotics, Jožef Stefan Institute, Ljubljana, Slovenia. jan.babic@ijs.si

Inspired by these biomechanical findings, robotics researchers have pursued both mechanical designs and motion control laws that emulate the function of biarticular muscles. Saito *et al* [10], [11] propose a biarticular actuation mechanism based on a bilateral servo system, and conduct experiments involving a bipedal robot as well as an externally powered orthosis. Tahara et al [12] show through simulation studies that biarticular actuation schemes, when endowed with the nonlinear and time-varying stiffness properties characteristic of muscles, can considerably simplify feedback control.

In work prior to this paper, Babic *et al* [13], [14] develop a planar jumping robot in which the thigh and ankle are connected by a biarticular link and spring-damper unit. Maximum height vertical jumping motions for this robot are also found under various simplifying assumptions, *e.g.*, contact with the floor is modeled as a rotational joint, the hip joint velocity is linearly related to the knee joint velocity, the ankle joint is active during contact but becomes passive when airborne, etc. The assumptions in [13] are made in large part to overcome the inherent complexities of modeling the dynamics of the biarticular jumping robot. The ensuing optimization must converge while ensuring that the dynamic equations are always satisfied.

While there is credible evidence suggesting that biarticular actuation schemes are indeed helpful for generating fast explosive movements, as yet we cannot make any quantifiable claims about the extent to which performance is improved—to do so the dynamics need to be accounted for in a complete way without any restrictive assumptions and simultaneous optimization with respect to both the actuator inputs and various parameters (*e.g.*, spring stiffness and the angle of the joint angle at which the passive biarticular link is activated) must be performed.

This paper attempts to determine in a quantifiable way the extent to how various parameters beyond the actuator input profiles, *e.g.*, stiffness, maximum force and velocity of the actuators, the angle of activation for biarticular structures, etc., improve movement performance. We make the following specific contributions:

Dynamic Modeling and Optimization of Biarticular Structures: In previous studies on dynamics-based motion optimization of both open and closed loop chains [15], [16], the advantages of analytic gradient-based motion optimization algorithms have been clearly demonstrated. For biarticular structures, several complexities not addressed in these previous studies arise: the dynamics model involves not only a closed chain with redundant actuation and spring elements, but also contact models between the feet and ground,

the optimization involves discontinuities at several levels (*e.g.*, the contact conditions, joints switching from passive to active, etc.) and diverse parameters in addition to the actuator inputs (*e.g.*, spring stiffness, activation angle, etc.). This paper extends the previous Lie theoretic gradient-based motion optimization algorithms to systems with biarticular actuation mechanisms, with corresponding objective functions for maximum height and maximum distance jumping. The algorithms show reliable convergence behavior over a wide range of robot structures and boundary conditions.

Evaluating the Effectiveness of Biarticular Structures: Using the optimization algorithms developed in this paper, we answer the question of exactly how effective biarticular mechanisms really are as a means of generating fast explosive movements in robots. Using the work of Babic *et al* [13], [14] as our point of departure, we make the following specific contributions:

- Most of the simplifying assumptions in the previous work are discarded;
- The biarticular system's optimized motions are compared with the corresponding optimal motions obtained for conventional and monoarticular robots;
- The effects of various mechanical design parameters such as spring stiffness and link masses on jumping performance are examined.

These results offer insight into how biarticular actuation schemes should be implemented in the design of high-performance biped robots, *e.g.*, minimum actuator requirements for a given desired level of performance. The optimized motions themselves can also be used as feedforward reference trajectories in the implementation of control laws for such systems.

This paper is organized as follows. In Section II we briefly review biarticular actuation mechanisms, and describe the planar jumping robot that will be the focus of our case studies. Section III describes the algorithm for generating optimal jumping movements, and provides a detailed analysis of these movements for our jumping robot. Section IV then discusses the effects of design values (spring stiffness, activation moment time) on jump performance based on a detailed case study for our robot. Section V concludes with a summary, and a brief discussion of the implications of our study on the design of next-generation robots that employ biarticular actuation.

II. Biarticular Leg Structure

Our model for a single planar jumping leg, consisting of four links serially connected by revolute joints, is shown in Figure 1. The base link of the robot is connected serially to the fixed reference frame by a set of virtual joints. A biarticular actuation mechanism is connected between the thigh and foot, passing through the knee and ankle joints.

Since our goal in this paper is to emulate the functional role of the biarticular muscle in improving jump performance, rather than to capture the exact muscle dynamic properties of biarticular gastrocnemius muscles, we express

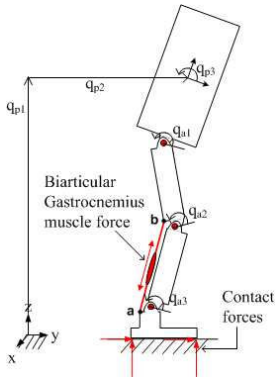

Fig. 1. Biarticular leg model.

the biarticular actuation force for our model as

$$f_{biarticular} = -k(x - x_0), \tag{1}$$

where x is the length of $b - a$, x_0 is the length of $b - a$ at the instant of activation, $b - a$ is a vector representing the direction of force, and k is the stiffness of the biarticular link. The instant at which the biarticular link is activated is specified by the angle of the knee joint θ_0: $x_0 = f(q_{a2}, q_{a3})_{q_{a2}=\theta_0}$, $\theta_0 = q_{a2,activation}$. The activation knee angle θ_0 and stiffness value k completely characterize the behavior of the biarticular actuation mechanism.

To better understand the biarticular actuation mechanism, consider a jumping motion starting from a squat position. Until the instant of activation, the biarticular actuation mechanism has no effect on the system, essentially acting as a passive prismatic joint. When the biarticular actuation mechanism is activated, the robot essentially becomes redundantly actuated by the biarticular force (one can think of a tension spring). Immediately after robot pushes off the ground, the biarticular actuator is deactivated. This sequence must be executed over a short time in an optimal fashion to maximize jump performance.

III. Movement Optimization Algorithm

Our planar jumping robot model is a floating body system in which the base link is not fixed. We can describe the base link motion using three virtual passive joints, two prismatic and one revolute, which are serially connected between the system base link and the fixed reference frame. The use of such a dynamic model employing passive virtual joints considerably simplifies the analysis and motion optimization, by allowing one to, *e.g.*, optimally determine the time at which the foot loses contact with the ground for maximum jumping performance, and rigorously taking into account frictional contact and collisions between the foot and ground.

Let $q = (q_a, q_p)$ be the set of coordinates describing the state of the overall system, where q_a and q_p denote the active and passive joints, respectively. The dynamic equations of motion for the system are then given by

$$M(q) \begin{pmatrix} \ddot{q}_a \\ \ddot{q}_p \end{pmatrix} + b(q, \dot{q}) = \begin{pmatrix} \tau_a \\ \tau_p \end{pmatrix} \tag{2}$$

where τ_a and τ_p are the torque (or force) vectors corresponding to q_a and q_p. The solution of such systems requires a hybrid dynamics algorithm such as the one suggested in [17], which in effect computes

$$(q_a, \dot{q}_a, \ddot{q}_a, q_p, \dot{q}_p, \tau_p) \rightarrow (\tau_a, \ddot{q}_p) \tag{3}$$

from repeated iterations of both the inverse and forward dynamics.

Accounting for both contact forces and biarticular muscle forces, the equations of motion assume the form

$$M(q) \begin{pmatrix} \ddot{q}_a \\ \ddot{q}_p \end{pmatrix} + b(q, \dot{q}) + J_c^T F_c + J_b^T F_b = \begin{pmatrix} \tau_a \\ \tau_p \end{pmatrix} \tag{4}$$

where F_c denotes the contact forces, F_b the biarticular forces (both F_c and F_b are expressed in generalized coordinates), and J_c and J_b are the respective Jacobians for position and orientation. To solve the above system equations under the action of frictional contact forces, we use Lemke's algorithm for the linear complementary problem (LCP) formulation, and also use the time-stepping schemes discussed in [18], [19] to reduce the integration error. The biarticular actuator force is assumed to exert an external force as prescribed by the muscle model equation (1).

Once the robot motion is determined from the corresponding active joint values $(q_a, \dot{q}_a, \ddot{q}_a)$ and the torques for the passive joints τ_p determined from kinematic information on the active joints, the joint accelerations $\ddot{q}_p$ of the passive joints can then be calculated, and the joint torques for the active joints determined via the hybrid dynamics equation. By numerical integration complete information on the passive joints $(q_p, \dot{q}_p, \ddot{q}_p)$ can be obtained. The robot motion can thus be described completely by joint angle position, velocity, and acceleration profiles for the active and passive joints. The active torque profiles required to execute the motion can also be calculated (note that our robot model has no passive joints excluding the three virtual passive joints, so that $\tau_p = 0$).

Given the above governing equations of motions, our goal is to optimize objective functions of the form

$$\begin{aligned} &\max_k \max_{q_a(t)} J = J(\tau_a, \tau_p, q_a, \dot{q}_a, \ddot{q}_a, q_p, \dot{q}_p, \ddot{q}_p, k) \\ &\text{subject to} \\ &\qquad \underline{q}_a \le q_a \le \overline{q}_a, \quad \underline{\dot{q}}_a \le \dot{q}_a \le \overline{\dot{q}}_a \\ &\qquad \underline{\tau}_a \le \tau_a \le \overline{\tau}_a, \quad \tau_p = 0 \\ &\qquad p_{com} \in \mathcal{P}_{com}, \quad p_{zmp} \in \mathcal{P}_{zmp} \end{aligned} \tag{5}$$

where p_{com} is the location of the center of mass of the robot, p_{zmp} is the zero moment point. Each joint trajectory is parameterized using quintic B-splines; the B-spline curve depends on the choice of basis functions $B_i(t)$, and the control points $P = \{p_1, \ldots, p_m\}$, with $p_i \in \Re^n$. The joint trajectories then assume the form $q = q(t, P)$, with

$$q(t, P) = \sum_{i=1}^{m} B_i(t) p_i \tag{6}$$

By parameterizing the trajectory in terms of B-splines, the original optimal control reduces to a parameter optimization problem, in which the optimization variables are the control points. Once the optimal control point values are determined, trajectories for the joint angle displacements, velocities, and accelerations can be derived straightforwardly from the B-spline basis functions. From that hybrid dynamics equation (2), the active torque values τ_a can be calculated. For our purposes we constrain τ_a using a penalty function; by constraining the internal active torque values it is possible to control the contact forces indirectly. Joint angle limits are easily bounded using B-spline properties; joint velocity limits can also be similarly constrained [20].

In the event that the biarticular link stiffnesses are assumed to have a fixed value, the objective function and constraints of Equation (5) can be expressed more concretely as

$$\begin{aligned} &\min_P J(P) = -J_{\text{performance}} + J_{\text{torque}} + J_{\text{posture}} \\ &\text{subject to} \\ &\quad p_0 = \cdots = p_4 = q_{a0}, \quad p_{m-3} = \cdots = p_m = q_{af} \\ &\quad \underline{q}_a \le p_i \le \overline{q}_a, \quad \underline{\dot{q}}_a \le \frac{(k-1)(p_j - p_{j-1})}{t_{j+k-1} - t_j} \le \overline{\dot{q}}_a \end{aligned} \tag{7}$$

where $J_{\text{performance}}$ represents a performance index to be maximize (*e.g.*, maximum height of the robot center of mass in the case of vertical jumping), J_{torque} is a penalty function bounding τ_a to within $[\underline{\tau}_a \, \overline{\tau}_a]$ *i.e.*,

$$J_{\text{torque}} = \sum_{0}^{t_f} (\underline{\tau}_a - \tau_a)^T (\underline{\tau}_a - \tau_a) + (\tau_a - \overline{\tau}_a)^T (\tau_a - \overline{\tau}_a), \tag{8}$$

and J_{posture} is a posture criterion to ensure that the robot does not fall over. The robot's initial and final states (as described by the displacement, velocity, and acceleration of the active joint angles) are easily set by adjusting the B-spline control points as in Equation (7); the posture can thus be checked by appropriately constraining the joint information corresponding the virtual passive joints (*e.g.*, $J_{\text{posture}} = (q_p(t_f) - c_1)^2$, or $(p_{com}(t_f) - c_2)^2$). By checking the final robot posture, it is possible to guarantee that the robot does not fall over during execution of the whole motion (because no external forces are exerted on the robot while in flight, it is impossible to recover posture without external power).

IV. Case Studies

This section considers two case studies involving (i) vertical jumping; and (ii) broad jumping. For the vertical jump case we determine the maximal height jumps for a given robot model, and also optimize the robot with respect to various design parameters (biarticular link stiffness, moment of activation, link masses). The nonlinear optimizations are executed using Matlab's Optimization Toolbox version 7.0 running on a Core 2 (2.13 GHz) personal computer. The stopping criterion $\mid J_{k+1}(P) - J_k(P) \mid < \epsilon$ with ϵ set to $10^{-3} \sim 10^{-5}$ is used for our optimizations.

A. Vertical Jump

We first consider maximum height vertical jumping movements for our biarticular model. Table I lists the kinematic and dynamic properties of the robot model used. An initial jumping motion is first generated via manual adjustment of control points, with the total jumping time set to 0.5 seconds.

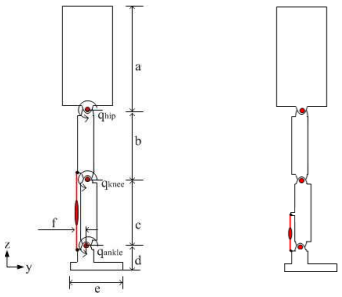

(a) Biarticular legged. (b) Monoarticular legged.

Fig. 2. Robot model.

TABLE I

ROBOT MODEL PARAMETERS.

Link	Length (mm)	COM (y,z)	Mass/Inertia (kg, kgmm^2)
Trunk	a=370	(100, 787.5)	(2.031, 20366)
Thigh	b=254	(100, 475.5)	(1.033, 7440)
Calf	c=255, f=30	(100, 221)	(0.963, 7487)
Foot	d=93.5, e=200	(100, 46.75)	(0.399, 1057)

Figure 3(a) shows the initial vertical jumping motion. The goal is to maximize the vertical height of the robot's center of mass at the final time t_f. Joint displacement and velocity limits can be imposed as simple linear inequality constraints on the B-spline control points. Limits on the actuated joint torques, and the selection of the final robot posture, are imposed by use of appropriate penalty functions to avoid the use of nonlinear constraints in the optimization.

The optimized vertical jumping motions are benchmarked with similar jumping motions for a conventional robot without biarticular actuation and also for a monoarticular robot as shown in Figure 2(b). We first consider the case of a biarticular actuated robot with biarticular link stiffness $k = 10000$ N/m and activation angle $\theta_0 = -90°$. The boundary conditions and constraints for the corresponding optimization are shown in Table II. The results of the optimization are

TABLE II

OPTIMIZATION PARAMETERS FOR VERTICAL JUMPING.

Optimization setting	(hip, knee, ankle)
Total jumping time (sec)	0.5
Integration sampling time (sec)	0.005
Friction coefficient	0.6
Number of variables	15
Performance index (max)	$J_{performance} = Height^2_{p_{com}(t_f)}$
Joint angle limits (rad)	$\overline{q} = (\pi, 0, \pi)$, $\underline{q} = (-\pi, -\pi, -\pi)$
Joint velocity limits (rad/sec)	$\overline{\dot{q}} = (20, 20, 20)$, $\underline{\dot{q}} = -\overline{\dot{q}}$
Joint torque limits (Nm)	$\overline{\tau} = (20, 20, 20)$, $\underline{\tau} = -\overline{\tau}$
Initial active joint values	$q_{a0} = (1.919, -2.094, 0.873)$
Final active joint values	$q_{af} = (0.175, -0.262, -1.047)$
Boundary conditions	$\dot{q}_{a0} = \ddot{q}_{a0} = \dot{q}_{af} = \ddot{q}_{af} = 0$

shown in Table III and Figure 3. Please see the accompanying video attachment to identify the corresponding optimized motions. As shown in Table III, the biarticulated robot reaches a maximum height that is nearly 23% higher than that of the conventional robot. Figure 4 shows the joint velocities/torques, normal contact forces, and mono-/biarticular link force trajectories for the optimized vertical jumps. It can be verified that the joint velocities and torques stay within the prescribed limits. A sudden and drastic increase in torque values for the biarticulated case can also be observed that cannot be generated by the actuators of the conventional robot. Figure 5 also shows the corresponding increase in power exertion for the optimized vertical jump. The apparent discontinuities in the torque profiles are due to changes in the contact state.

TABLE III

OPTIMIZATION OF VERTICAL JUMP

	Conventional	Mono-	Bi-articulated
Maximum jump height (m)	0.1230	0.1294	0.1509
Optimization time (min.)	38.7	38.05	37.79

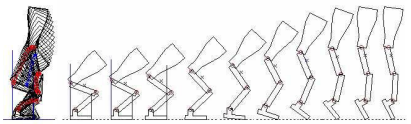

(a) Initial motion.

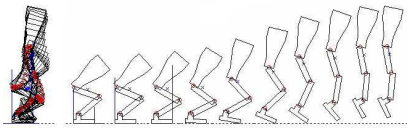

(b) Optimized motion for the conventional robot.

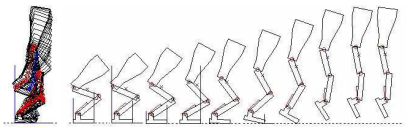

(c) Optimized motion for the monoarticular legged robot (k=10000 N/m, θ_0=$-90°$).

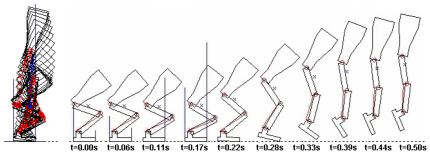

(d) Optimized motion for the biarticular legged robot (k=10000 N/m, θ_0=$-90°$).

Fig. 3. Vertical jump.

As shown in Figure 4, the maximum torque in the ankle joint is lower in the system with the biarticular actuator compared to the conventional and monoarticular cases. At the end of the stance phase, when the biarticular element exerts a force, the torques in the proximal joints, hip, and knee increase, while the torque in the ankle decreases. This phenomenon can be traced to power transfer from the proximal joints to the distal joints delivered via the biarticular element. This effect allows one to implement an actuator in the ankle joints that has a lower maximum torque compared to the knee and hip actuators. The smaller ankle motor is

generally associated with a lower weight; hence, the mass of the calf and foot can be reduced. The further results of this study in Tables VI and VII show that a lower weight of the distal elements (calf and foot) leads to higher jumping performance, even for the cases when the upper segments are made slightly heavier.

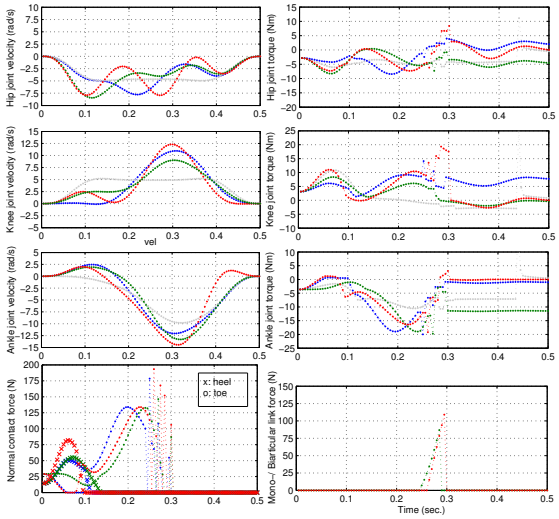

Fig. 4. Joint velocities/torques, normal contact forces, and biarticular force trajectories for optimized vertical jumps (gray: initial motion, blue: conventional robot, green: monoarticular legged robot, red: biarticular legged robot).

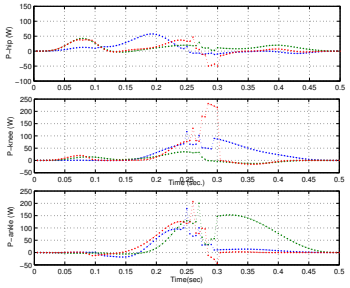

Fig. 5. Joint power profiles for optimized vertical jumps (blue: conventional robot, green: monoarticular legged robot, red: biarticular legged robot).

TABLE IV

ACTIVATION MOMENT ANGLE OPTIMIZATION FOR SELECTED STIFFNESS.

	Jump height (m)		
Activation angle (°)	k=5000	k=10000	k=15000
-70	0.0758	0.0753	0.0997
-80	0.1025	0.0758	**0.1128**
-90	**0.1242**	**0.1509**	**0.1140**
-100	**0.1503**	**0.1297**	0.1066
-110	0.0757	0.1121	0.0889

1) Activation angle optimization: We also optimize the vertical jumping motion with respect to the activation angle, *i.e.*, the angle at which the biarticular actuation is applied. The results are shown in Table IV; it can be observed that the optimal activation angle lies in the range $-90 \sim -100°$. Not surprisingly the precise values depend on the choice of biarticular link stiffness values.

TABLE V

STIFFNESS OPTIMIZATION FOR SELECTED ACTIVATION ANGLES.

	Jump height (m)		
Stiffness (N/m)	$\theta_0 = -80°$	$\theta_0 = -90°$	$\theta_0 = -100°$
5000	0.1025	0.1242	**0.1503**
7000	0.1241	**0.1651**	0.1105
9000	**0.1491**	0.1242	0.1074
11000	0.0759	0.1250	0.0982
13000	0,0949	0.0758	0.1134

2) Stiffness optimization: We now optimize the biarticular link stiffness values for a prescribed set of activation angles; the results are shown in Tables IV and V; the results show that the maximum height attained is clearly higher for the biarticulated robot than for the conventional robot (0.123 m). Table V indicates that for our particular biarticulated robot model, the maximum height for prescribed stiffness value 7000 N/m is attained when $\theta_0 = -90°$.

TABLE VI

SELECTED LINK MASSES SET (kg).

Link	I	II	III	IV	V
Trunk	2	3	1.1	0.4	2
Thigh	1	0.5	1.1	1	0.6
Calf	1	0.5	1.1	1	0.4
Foot	0.4	0.4	1.1	2	1.4

3) Effects of link masses on vertical jumping: We now examine the effects of the choice of link masses on the vertical jump height. Table VI shows five different sets of choice of link masses; for each set we determine the maximum vertical jumping height via our optimization algorithm. Note that the total robot is constrained to be a constant 4.4 kg in all five cases. The results of the optimization are given in Table VII. As can be seen for the results obtained for case IV, a heavy foot is clearly disadvantageous for jumping, and having the mass concentrated in the trunk is more helpful. On the other hand, in most current humanoid robots it is not uncommon to see actuators with more or less similar specifications used at each joint, and from this perspective having the mass concentrated in one particular link can be disadvantageous. Our results indicate that link masses have a strong influence on vertical jumping motions, particularly for conventional robots (the effects are less pronounced for biarticular robots, allowing for a greater range of mass distributions over the links for biarticulated structures). The best result is obtained for the biarticulated case II.

B. Broad jump

We now generate maximum distance broad jumps for both the biarticulated and conventional robot structures. For the biarticular mechanism, the link stiffness is set to $k = 5000$ N/m, and the activation angle to $\theta_0 = -80°$. The boundary

TABLE VII

MAXIMUM HEIGHT JUMPS FOR SELECTED LINK MASSES.

	Jump height (m)	
Link masses set	Conventional robot	Biarticulated robot
I	**0.1287**	0.1307
II	0.0753	**0.1921**
III	0.0854	0.1057
IV	0.0752	0.0756
V	0.0755	0.1390

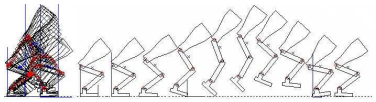

(a) Initial motion.

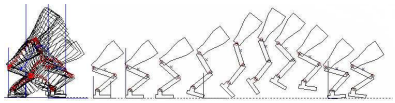

(b) Optimized motion for the conventional robot.

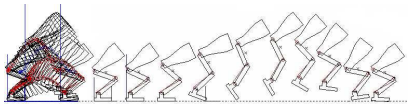

(c) Optimized motion for the biarticular legged robot(k=5000 N/m, θ_0=$-80°$).

Fig. 6. Broad jump.

TABLE VIII

MAXIMUM DISTANCE BROAD JUMP.

	Conventional robot	Biarticulated robot
Maximum distance (m)	0.4768	0.5695
Optimization time (min.)	40.89	57.26

conditions and constraints for the broad jump are the same as those used for vertical jumping, except for the final posture and total jumping time (set to $t_f = 0.8$ sec in the case of the broad jump). The results of the optimization are shown in Table VIII and Figure 6. For the particular choice of model, the maximum distance achieved by the biarticulated robot is nearly 20% more than that of the conventional robot.

V. CONCLUSION

This paper has examined the extent to which biarticular mechanisms can improve the jumping performance of legged structures. After developing detailed planar dynamic models of biarticular legged structures, we formulate the ensuing optimization problems for maximum height vertical jumping and maximum distance broad jumping. Case studies involving a four degree-of-freedom biarticular leg structure are compared with those for an identical structure without biarticular actuation, and a quantitative comparison performed for the two cases. Our results indicate that biarticular actuation not only considerably improves jumping performance (by up to 25%), but that the resulting performance gains are less affected by, *e.g.*, the choice of link mass distributions. Current research is directed at performing experiments with a hardware prototype of a biarticular jumping robot [21]. Future work on movement optimization with spatial dynamic models, involving more complex movements such as running high jumps and hurdling, is underway.

REFERENCES

[1] R. Hayashi, and S. Tsujio, "High-performance jumping movements by pendulum-type jumping machines," *Proc. IEEE/RSJ Int. Conf. Intel. Robots and Systems*, pp. 722-727, 2001.

[2] Y. Saito, T. Nagano, T. Seki, M. Ishikawa, and S. Hara, "Optimal high-jump control of linear 1-d.o.f trampoline robot," *Proc. 41st SICE Annual Conf.*, pp. 2527-2530, 2002.

[3] K. Arikawa and T. Mita, "Design of multi-DOF jumping robot," *Proc. IEEE Int. Conf. Robotics Autom.*, pp. 3992-3997, 2002.

[4] S. Sakka and K. Yokoi, "Humanoid vertical jumping based on force feedback and inertial forces optimization," *Proc. IEEE Int. Conf. Robotics Autom.*, pp. 3752- 3757, 2005.

[5] J.V. Albro, and J.E. Bobrow, "Optimal motion primitives for a 5-DOF experimental hopper," *Proc. IEEE Int. Conf. Robotics Autom.*, pp. 3630-3635, 2001.

[6] F.C. Anderson and M.G. Pandy, "A dynamic optimization solution for vertical jumping in three dimensions," *Comp. Methods Biomech. Biomed. Eng.*, vol. 2 pp. 201-231, 1999.

[7] R. Jacobs, M.F. Bobbert, and G.J. van Ingen Schenau, "Mechanical output from individual muscles during exposive leg extensions: the role of biarticular muscles," *J. Biomechanics*, vol. 29, no. 4, pp. 513-523, 1996.

[8] M.R. Shorten, "Mechanical energy changes and elastic energy storage during treadmill running," in *Biomechanics IXB*, D. Winter, R. Norman, R. Well, K. Hayes, and A. Patla, Eds., *Human Kinetics*, Champaign, Ill., pp. 65-70, 1985.

[9] K. Kubo, Y. Kawakami, and T. Fukunaga, "Influence of elastic properties of tendon structures on jump performance in humans," *J. Applied Physiology*, vol. 87, no. 6, pp. 2090-2096, 1999.

[10] Y. Saito, K. Kikuchi, H. Negoto, T. Oshima, and T. Haneyoshi, "Development of externally powered lower limb orthosis with bilateral-servo actuator," *Proc. Int. Conf. Rehabilitation Robotics*, pp. 394-399, 2005.

[11] Y. Saito, T. Matsuoka, and H. Negoto, "Study on designing a biped robot with bi-articular muscle type bilateral servo system," *Proc. Int. Workshop Robots and Human Interactive Communication*, pp. 490-495, 2005.

[12] K. Tahara, Zhi-Wei Luo, and S. Arimoto, "On control mechanism of human-like reaching movements with musculo-skeletal redundancy," *Proc. IEEE/RSJ Int. Conf. Intel. Robots and Systems*, pp. 1402-1409, 2006.

[13] J. Babic, and J. Lenarcic, "Optimization of biarticular gastrocnemius muscle in humanoid jumping robot simulation," *Int. J. Humanoid Robotics*, vol. 3, no. 2, pp. 219-234, 2006.

[14] J. Babic, D. Omrcen, and J. Lenarcic, "Balance and control of human inspired jumping robot," in *Advances in Robot Kinematics: Mechanisms and Motion*, J. Lenarcic and B. Roth, Eds., Dordrecht, Springer, pp. 147-156, 2006.

[15] J.E. Bobrow, B. Martin, G. Sohl, E.C. Wang, F.C. Park, and J. Kim, "Optimal robot motions for physical criteria," *J. Robotic Systems*, vol. 18, no. 12, pp. 785-795, 2001.

[16] S. Lee, J. Kim, F.C. Park, Munsang Kim, and J.E. Bobrow, "Newton-type algorithms for dynamics-based robot motion optimization," *IEEE Trans. Robotics*, vol. 21, no. 4, pp. 657-667, 2005.

[17] J. V. Albro, G.A. Sohl, J. E. Bobrow, and F. C. Park, "On the computation of optimal high-dives," *Proc. IEEE Int. Conf. Robotics Autom.*, pp. 3958-3963, April 2000.

[18] M. Anitescu, and F.A. Potra, "Formulating dynamic multi-rigid-body contact problems with friction as solvable linear complementarity problems," *Nonlinear Dynamics*, vol. 14, pp. 231–247, 1997.

[19] F. A. Potra, M. Anitescu, B. Gavrea, and J. Trinkle, "A linearly implicit trapezoidal method for integrating stiff multibody dynamics with contact, joints and friction," *Int. J. Numer. Meth. Engineering*, vol. 66, no. 7, pp. 1079-1124, 2006.

[20] C.Y.E. Wang, W.K. Timoszyk, and J.E. Bobrow, "Weightlifting motion planning for a Puma 762 robot," *Proc. IEEE Int. Conf. Robotics Autom.*, pp. 480-485, May 1999.

[21] J. Babic, Bokman Lim, D. Omrecen, and F.C. Park, "Design and movement optimization for biarticular legged robots: Theory and experiments,"*Advanced Robotics*, 2007 (under review).